Strain-induced change of surface reconstructions for InAs(001)

C. Ratsch*

Department of Mathematics, University of California, Los Angeles, California 90095-1555
and HRL Laboratories LLC, 3011 Malibu Canyon Road, Malibu, California 90265

The effect of strain on the stability of different surface reconstructions on InAs(001) is investigated with density-functional theory calculations. The effects of isotropic as well as anisotropic tensile and compressive strain is investigated, and the results are presented in corresponding equilibrium phase diagrams. I find that the range of stability for any of the relevant reconstructions can be changed significantly, and, in fact, a reconstruction that is unstable in an unstrained system might be stabilized upon application of external strain.

Many high speed and optoelectronic devices are based on III-V compound semiconductor systems. In the quest for better and faster performance, these devices are becoming progressively smaller. With the decreasing size of such a quantum layer semiconductor device, the thickness and also the morphology of the interface between different heterolayers can be of crucial importance. Thus, many theoretical efforts focus on understanding of the growth dynamics for adatoms (group III and V) on these surfaces, so that the morphology of the surfaces and thus of the interfaces can be controlled.

It is well known that experimental conditions such as deposition flux and temperature determine the reconstruction on the surface during epitaxial growth,[1] which in turn influences the adatom dynamics on the surface. In previous calculations for InAs(001),[2,3] it has been predicted that there are (at least) four stable surface reconstructions on this surface: With increasing chemical potential for As, μ_{As}, they are the $\alpha 3(2\times4)$, $\alpha 2(2\times4)$, $\beta 2(2\times4)$, and $c(4\times4)$ reconstructions. For reference, the resulting phase diagram from Ref. 3 for InAs(001) without external strain is shown in Fig. 1. The relevant surface reconstructions are shown in Fig. 2.

In this paper I investigate how the surface reconstruction on InAs(001) can be altered upon application of external strain. Strain is important, since many heterostructures consist of layers that have different lattice constants. If these materials with different lattice constants are grown epitaxially, this leads to strain in the system. The effect of strain on the surface reconstruction has, for example, been studied by Swartzentruber *et al.*[4] for Si(001). The authors showed that it is possible to systematically bend a substrate in a growth chamber, thus changing the surface reconstruction. A similar experiment for InAs(001) might offer the possibilities to study systematically the results presented in this study.

The calculations are similar to those that have been described in Ref. 3. I study tensile as well as compressive strain, and for all the results shown below, the value chosen is 4%. This value is large enough to illustrate the effect of strain, but small enough to allow growth of coherently strained thin layers (without the introduction of dislocations). It is of the order of the mismatch between AlAs and In$_{0.5}$Ga$_{0.5}$As, which is a material combination used for resonant tunneling diodes, and which, in fact, has been grown coherently strained for up to six monolayers.[5] It is also smaller than the lattice mismatch of 7% between InAs and

GaAs, which are the most widely studied III/V semiconductor systems. Some test calculations indicate that for lesser values of strain the effects discussed here are also present, but are correspondingly smaller. For the (2×4) reconstructions, the As dimers are oriented in the $[\bar{1}10]$ direction, while the In dimers are oriented along the $[110]$ direction. It is a reasonable to expect that strain along the $[\bar{1}10]$ direction will have a different effect than strain along the $[110]$ direction. Therefore, results for isotropic and anisotropic (in both, the $[\bar{1}10]$ and $[110]$ direction) strain are presented.

The stable surface reconstruction is determined as the one with the lowest surface free energy density, γ. For a system with two chemical species, the surface energy of an area A with N_i atoms of species i is given by

$$\gamma A = E_{surf} - \sum_i \mu_i N_i, \qquad (1)$$

where the chemical potential μ_i is the energy required to extract an atom of species i from a corresponding reservoir. The chemical potentials are related to the experimental conditions; a higher value of the chemical potential μ_{As} (μ_{In}) corresponds to more As (In) rich conditions. The values for μ_i are bounded by their respective bulk values $\mu_{In}^{(b)}$ and $\mu_{As}^{(b)}$. Additionally, the equilibrium condition $\mu_{In} + \mu_{As} = \mu_{InAs}$ must be satisfied, otherwise the system would adjust
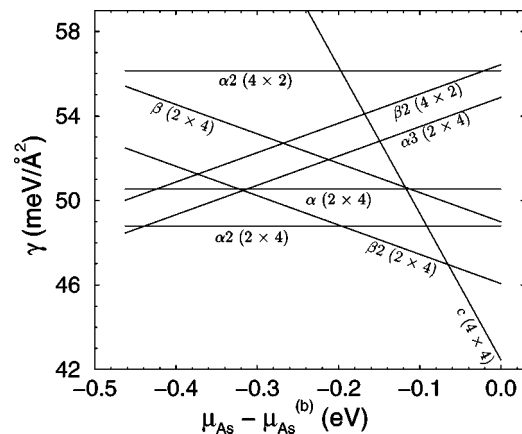

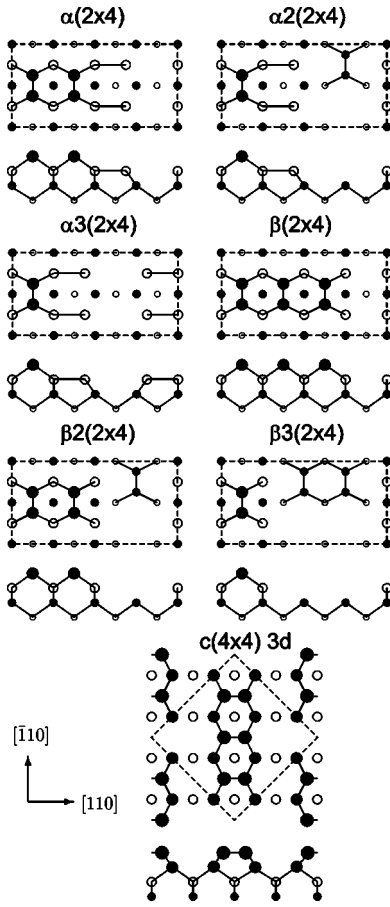FIG. 1. Equilibrium phase diagram for InAs(001) without external strain calculated with DFT.

63 161306-1

FIG. 2. Schematic representation of the relevant (2×4) structures and the $c(4\times4)$ with three top As dimers (3d). Closed (open) circles represent As(In) atoms, and the size reflects the height. The corresponding (4×2) structures are rotated by 90°, with In and As atoms exchanged. Shown are top and side views. The crystallographic directions indicated refer to the top view.
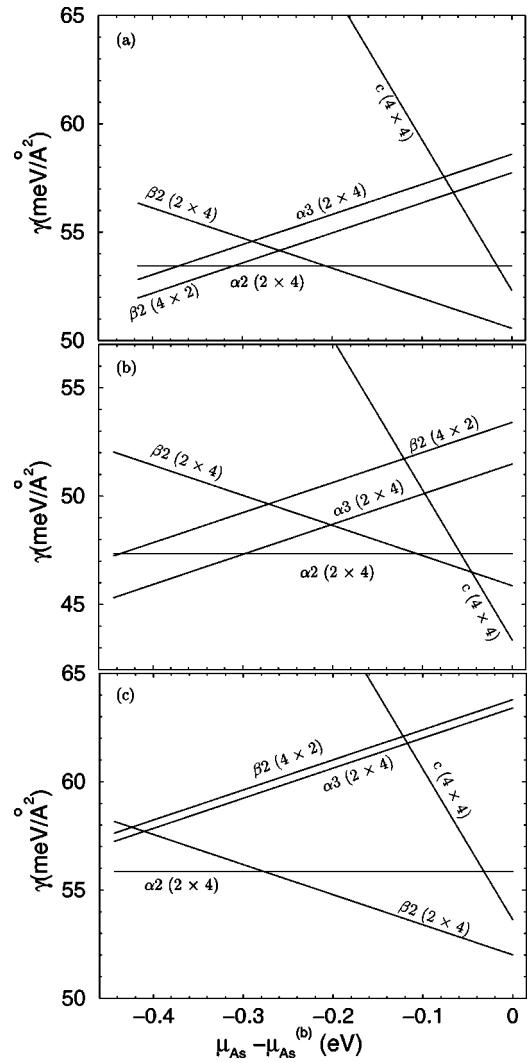

FIG. 3. Equilibrium phase diagram for InAs(001) calculated with DFT for (a) 4% isotropic tensile strain, (b) 4% tensile strain along the $[\bar{1}10]$ direction, and (c) 4% tensile strain along the $[110]$ direction.

by forming more (or less) InAs bulk. The chemical potential μ_{InAs} is the energy per InAs pair in InAs bulk.

The energy E_{surf} and the chemical potentials μ_i were obtained from density-functional theory (DFT) calculations. I employed the local-density approximation (LDA) and used norm-conserving pseudopotentials[6,7] as implemented in the computer code FHI98MD.[8] The electronic wave functions were expanded in a plane-wave basis that was truncated at a cutoff energy of $E_{\mathrm{cut}}=12$ Ry. For the **k** summation I used the equivalent of 8×8 points in a (1×1) cell that were generated according to the scheme proposed by Monkhorst and Pack.[9] All structures were calculated in a unit cell of size (2×4) [or (4×2)] and a slab thickness of eight (or seven) atomic layers, so that the bottom layer was terminated by a layer of group III atoms. The dangling bonds were then saturated with pseudohydrogen atoms of charge 1.25. A vacuum separation equivalent to ten atomic layers was chosen. All atoms were allowed to relax, except the bottom layer of In and As. Thus the computational parameters for the calculations for the strained systems are essentially the same as those for the unstrained system.[3] The chemical potentials $\mu_{\mathrm{In}}^{(b)}$ and $\mu_{\mathrm{As}}^{(b)}$ are obtained from calculations of In and As

bulk cells. For a strained system, the chemical potential μ_{InAs} is not the bulk energy for unstrained InAs. I therefore calculated the energy of pseudobulk systems, that are strained anisotropically either in the $[\bar{1}10]$ or $[110]$ direction, or isotropically in both directions, while at the same time the system was allowed to relax in the $[001]$ direction.

The resulting equilibrium phase diagrams for tensile and compressive strain are shown in Figs. 3 and 4. The reconstructions that are considered here are the ones that are stable without strain, and, in addition, the $\beta2(4\times2)$, which is believed to play a role in the As deficient growth regime. Unless stated otherwise, the discussion of each of the panels is always in reference to the unstrained system, as shown in Fig. 1.

I begin the discussion by focusing on the results for isotropic strain [Figs. 3(a) and 4(a)]. For tensile isotropic strain [Fig. 3(a)], the range of stability of the $\beta2(2\times4)$ is extended, in particular under As rich condition at the expense of the $c(4\times4)$ reconstruction. The range of stability of the
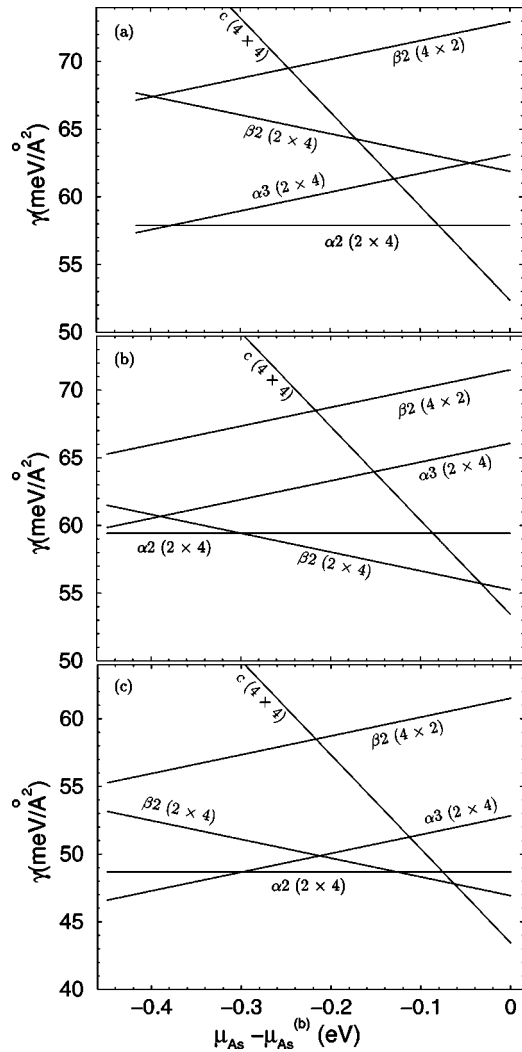
FIG. 4. Equilibrium phase diagram for InAs(001) calculated with DFT for (a) 4% isotropic compressive strain, (b) 4% compressive strain along the $[\bar{1}10]$ direction, and (c) 4% compressive strain along the [110] direction.

constraints due to the underlying zinc-blende lattice structure. Thus, tensile strain along a dimer will weaken a dimer bond, while compressive strain will strengthen it. However, it is not clear how much the strength of the dimer bonds will be changed, or how strain will affect all the other bonds.

Many features of the effect of isotropic tensile strain are reproduced by tensile strain along the [110] direction. This can be seen by comparing Fig. 3(a) (isotropic tensile strain) and Fig. 3(c) (tensile strain along the [110] direction). In both cases, the stability of the $\beta2(2\times4)$ is extended at the expense of the $c(4\times4)$ reconstruction. The As dimers for the $c(4\times4)$ reconstruction are oriented along the [110] direction, while the As dimers for all the (2×4) reconstructions considered here are along the $[\bar{1}10]$ direction. Thus, tensile strain along the [110] direction is particularly disadvantageous for the $c(4\times4)$ reconstruction, thus favoring the $\beta2(2\times4)$.

Tensile isotropic strain only slightly weakens the In dimer bonds for the $\beta2(4\times2)$ reconstruction, and has very little effect on the underlying In-As bonds. In contrast, it weakens the In dimer bonds and In-As bonds of the $\alpha3(2\times4)$ reconstruction, by lengthening them by 1% and 2%, respectively. Thus, the net effect of tensile strain is to stabilize the $\beta2(4\times2)$ reconstruction. The effect is not quite that pronounced for tensile strain along the [110] direction, since here the As dimer for the $\alpha3(2\times4)$ (that is oriented along the $[\bar{1}10]$ direction) is not affected. Therefore, tensile strain along the [110] results in the $\alpha3(2\times4)$ and $\beta2(4\times2)$ structures being essentially degenerate in energy. However, tensile strain along the $[\bar{1}10]$ *and* [110] directions reverses the order of the $\alpha3(2\times4)$ and $\beta2(4\times2)$, and, in fact, stabilizes the $\beta2(4\times2)$ reconstruction.

Tensile strain along the $[\bar{1}10]$ direction appears to affect all structures similarly [Fig. 3(b)], and results in a phase diagram that is almost identical to the one obtained without strain. This is a little surprising, as one would expect that the As dimers along the $[\bar{1}10]$ direction should be destabilized. This does not happen, however, and their bond lengths are within 0.5% of the value for the unstrained system.

The results for compressive strain are shown in Fig. 4. The most striking observation for isotropic compressive strain is that the stable regime of the $\alpha2(2\times4)$ is extended significantly [Fig. 4(a)]. This can be understood as follows: All dimer bonds (In dimers and As dimers) are stabilized by compressive strain. This observation by itself does not explain why some structures might be more favored than others, since all structures have dimers. However, it turns out that under compressive strain the In-In dimer bonds are shortened (and thus stabilized) most. For the $\alpha2(2\times4)$ reconstruction, the In-In dimer is shortened by $\sim3\%$. Since this bond is oriented in the [110] direction, it is also stabilized [at the expense of the $\beta2(2\times4)$] for compressive strain only along the [110] direction, as can be seen in Fig. 4(c). The $\alpha3(2\times4)$ has 4 In-In dimers along the [110] direction. Thus, this reconstruction is particularly favored under compressive isotropic strain along this direction.

These calculations could explain the results of Belk *et al.*[10] which show that for InAs on GaAs(001) (a system

$\alpha2(2\times4)$ is much shorter than in the unstrained case. This is in sharp contrast to the results for compressive isotropic strain, where in fact the $\beta2(2\times4)$ is not stable at all, and the $\alpha2(2\times4)$ reconstruction is the preferred one over almost the entire regime. Another interesting feature is that tensile strain reverses the order of the $\alpha3(2\times4)$ and the $\beta2(4\times2)$ reconstruction. As a reminder, there is no (4×2) reconstruction found in calculations for the unstrained system that is stable (even though it is observed in experiments). I find that tensile isotropic strain stabilizes the $\beta2(4\times2)$ reconstruction. In contrast, for compressive strain the energy gap between the $\alpha3(2\times4)$ and the $\beta2(4\times2)$ is even wider.

The results described above can be better understood if one studies the change in the phase diagrams upon anisotropic strain. In particular, I will analyze how strain (both tensile and compressive) along a dimer (i.e., along the axis that connects the dimer atoms) affects the surface reconstruction. All the dimer bonds for the structures discussed here are already under tensile strain, which is a result of geometric

with 7% compressive strain) the $\beta2(2\times4)$ reconstruction disappears. The authors find that upon decrease of the As overpressure, the surface reconstruction changes from a (4 $\times$4) reconstruction to a (1$\times$3) reconstruction, without the appearance of the $\beta2(2\times4)$ reconstruction. The results presented here suggest that this is the case because the $\beta2(2\times4)$ is particularly unfavored upon isotropic compressive strain.

It is interesting to note that the effect of compressive strain along the [110] direction [Fig. 4(c)] is almost the same as tensile strain along the [$\bar{1}$10] direction [Fig. 3(b)]. This can be explained as follows: In both cases, the In-In dimers become more stable in comparison to the As-As dimers, since the In-In dimers are stabilized under compressive strain along the [110] direction, while the As-As dimers are destabilized under tensile strain along the [$\bar{1}$10] direction. Similarly, compressive strain along the [$\bar{1}$10] direction and tensile strain along the [110] direction can be compared. Compressive strain along the [$\bar{1}$10] direction favors the As dimers in the (2$\times$4) reconstruction, but has essentially no effect on the In-In dimer bonds. Thus, compressive strain along the [$\bar{1}$10] direction extends the regime of stability of the $\beta2(2\times4)$ reconstruction [Fig. 4(b)]. This is similar to

the results of tensile strain along the [110] direction [Fig. 3(c)], since here mainly the In-In dimer bonds [that are present in the $\alpha2(2\times4)$, $\alpha(2\times4)$, and $\beta2(4\times2)$ reconstructions] are weakened (stretched by ~2%).

The calculations presented here show that strain that arises in heteroepitaxial growth changes the stability of surface reconstructions. Also, strain might be used as an additional parameter during epitaxial growth to control the morphology of a growing film. For example, growth on a (4 $\times$2) often leads to films of poor quality, presumably because the excess In atoms form droplets on the surface. However, the present calculations suggest that under tensile strain, the $\beta2(4\times2)$ reconstruction is stable under more As rich conditions, and thus it is less likely that In-droplets form on this In-terminated surface. For many materials systems, strain as an additional parameter during growth might help to grow new structures, or to characterize a surface structure.

*Electronic address: cratsch@math.ucla.edu

[1] H. Yamaguchi and Y. Horikoshi, Phys. Rev. B **51**, 9836 (1995).

[2] E. Pehlke, N. Moll, A. Kley, and M. Scheffler, Appl. Phys. A: Mater. Sci. Process. **65**, 525 (1997).

[3] C. Ratsch, W. Barvosa-Carter, F. Grosse, J. H. G. Owen, and J. J. Zinck, Phys. Rev. B **62**, R7719 (2000).

[4] B. S. Swartzentruber, Y. W. Mo, M. B. Webb, and M. G. Lagally, J. Vac. Sci. Technol. A **8**, 210 (1990).

[5] D. H. Chow, M. Hafizi, W. E. Stanchina, J. A. Roth, J. J. Zinck, J.-J. Dubray, and H. L. Dunlap, J. Vac. Sci. Technol. B **16**, 1413 (1998).

[6] D. R. Hamann, Phys. Rev. B **40**, 2980 (1989).

[7] M. Fuchs and M. Scheffler, Comput. Phys. Commun. **119**, 67 (1999).

[8] M. Bockstedte, A. Kley, J. Neugebauer, and M. Scheffler, Comput. Phys. Commun. **107**, 187 (1997).

[9] H. J. Monkhorst and J. D. Pack, Phys. Rev. B **13**, 5188 (1976).

[10] J. G. Belk, C. F. McConcille, J. L. Sudijono, T. S. Jones, and B. A. Joyce, Surf. Sci. **387**, 213 (1997).